ЖЭТФ, 2019, том 155, вып. 1, стр. 62–68

TOWARDS SOLVING THE MASS-COMPOSITION PROBLEM IN ULTRA HIGH ENERGY COSMIC RAYS

R. Aloisio [a,b*], ***V. Berezinsky*** [a,b**]

[a] *Gran Sasso Science Institute*
67100, L'Aquila, Italy

[b] *INFN — Laboratori Nazionali Gran Sasso*
67100, Assergi (AQ), Italy

Received April 27, 2018,
revised version July 5, 2018.
Accepted July 5, 2018

DOI: 10.1134/S004445101901005X

1. INTRODUCTION

Mass composition still remains a controversial issue in ultra high energy cosmic rays (UHECR). The three biggest detectors, Pierre Auger (referred here as "Auger"), Telescope Array (referred as "TA") and HiRes, have obtained contradictory results concerning mass composition of primary particles in the energy range 3–100 EeV (1 EeV $= 1 \cdot 10^{18}$ eV). At 1–3 EeV all three detectors agree with light composition, protons or protons and Helium, but in the range 3–100 EeV the Auger detector, the biggest one, founds a progressively heavier mass composition with increasing energy, while the other two detectors report the mass composition similar to that at lower energy.

At present there are two basic methods to study the mass composition of UHECR: direct measurements and indirect tests. The more reliable direct method is based on the observation of the fluorescent light produced by extensive air showers (EAS) in the atmosphere. The indirect test is based on the signatures of mass composition in the primary energy spectrum and we start with it as more old and less constraining.

This approach works most efficiently for protons due to their interaction with the cosmic microwave background (CMB). It results in two very specific spectral features: the Greisen–Zatsepin–Kuzmin (GZK) cutoff [1] and the pair-production dip. The former is a sharp cutoff at the end of the spectrum, around $E \approx 50$ EeV, due to the photo-pion production and the latter is a rather faint feature at $E \sim$ 1–30 EeV first calculated in [2] and studied in detail in [3–5]. The dip is well confirmed in the spectra of all three detectors but its origin as the pair-production dip $p + \gamma_{cmb} \to p + e^- + e^+$ is now questioned by the Auger mass composition. Before 2011 the data published by HiRes [6] and Auger [7], and later confirmed by TA, showed high energy steepening in good agreement with the predicted GZK cutoff.

The propagation of UHE nuclei does not leave any clear signature of the mass composition in the energy spectra. The main channel of energy losses, that determines the spectrum of UHE nuclei is the photo-disintegration process on the extragalactic background light (EBL) and on CMB. This process naturally produces the secondary lighter nuclei, mixing thus with the primary composition. As was first predicted by Gerasimova and Rozental [8] in 1961, i. e. before the discovery of CMB, nuclei photo-disintegration on EBL results in a suppression of the UHECR energy spectrum (GR steepening). In fact, as was realised later, see e. g. [9], a more sharp cutoff occurs at higher energies where the nucleus photo-disintegration time on CMB becomes equal to that on EBL. This cutoff arises at Lorenz-factor $\Gamma \sim (3\text{–}5) \cdot 10^9$ for all nuclei. The energy of the cutoff $E_{cut} \propto A\Gamma$ is different for primary nuclei with different A. This fact together with the unavoidable mixed composition, due to the production of secondary nuclei makes unclear any composition signature in the observed spectrum.

At present the best method to measure the mass composition is given by the observation of fluorescent light produced by the electromagnetic component of EAS in the atmosphere. All three aforementioned detectors use this method. However, for better accuracy

* E-mail: roberto.aloisio@gssi.it
** E-mail: berezinsky@lngs.infn.it

the fluorescent-light method needs additional information, which in the case of HiRes is given by the stereo observation of fluorescent light, and in the case of Auger (and recently of TA) this additional information is obtained from the data of on-ground detectors (water-Cherenkov detectors in Auger and scintillation detectors in TA).

The basic observable parameter related to mass composition is $X_{max}(E)$, the atmospheric depth where the number $N(E)$ of particles in the cascade, with total energy E, reaches its maximum. X_{max}, is sensitive to the number of nucleons in the primary nucleus. Heavy nuclei interact higher in the atmosphere and have smaller fluctuations. In practice the actual quantity which allows to find the mass composition is the distribution $N(X_{max})$ of the showers with total energy E.

In the case of large statistics the direct use of $N(X_{max}, E)$ gives the most reliable estimation of composition. In the case of limited statistics one may use the moments of this distribution, see e. g. [10], namely the first moment which is the mean value $\langle X_{max}\rangle$ and the second moment $\sigma(X_{max})$ which is the variance or dispersion (RMS) of the distribution. As was demonstrated in [11] using only the first two moments for the analysis, may result in a false degeneracy: two different mass compositions may produce the same $\langle X_{max}\rangle$ and $\sigma(X_{max})$.

The shape-fitting analysis of $N(X_{max})$ recently performed by the Auger collaboration [11] gives very important results that, summarising, can be described as follows. The mass composition is assumed as a discrete sum of four elements: Iron (Fe), Nitrogen (N), Helium (He) and protons (p). For each element the X_{max} distribution is calculated by Monte Carlo (MC) simulations and the fraction of each element in the total flux is found from the comparison with observations. These fractions depend on the models of hadronic interaction included in MC simulations. A decisive result is given by the very small fraction of Iron at all energies, almost independently of the hadronic interaction model (see the upper panel of Fig. 4 in [11]). Besides, the analysis of [11] shows that the fraction of light elements (p+He) is quite large independently of the hadronic interaction model. It allows the conclusion that at least a large fraction of UHECR, if not the dominant one, is composed by light elements. The small fraction of Iron and large of p + He seem to be a common conclusion of the $N(X_{max})$ shape-fitting analysis of Auger and HiRes/TA data.

The argument above does not dismiss the question: Auger, HiRes and TA use the same fluorescent data to measure X_{max} and the same moments-based method for the analysis of mass composition. Why then their conclusions differ? The most convincing answer to this question is probably given in a recent paper by the TA collaboration [12]. The observation of fluorescence light can be performed in two ways: with a monocular observation, when only one telescope observes the fluorescent signal, or in the stereo mode when more than one telescope simultaneously observe the same shower. Fluorescence detection in monocular mode is less efficient to measure X_{max} in comparison with the stereo mode. HiRes and later TA used, apart from monocular, also stereo events with higher precision in the measurement of X_{max}. It became possible because of the smaller (in comparison with Auger) spatial separation between telescopes. Auger, on the other side, to cover a larger area has a much larger separation among telescopes and collected mainly monocular fluorescent events. Instead, the Auger collaboration elaborated the hybrid technique, first proposed in [13], based on additional accompanying signal from, at least, one on-ground water-Cherenkov detector. Hybrid method allows to measure the core location and geometry of the shower, which improve the measurement precision for X_{max} and shower energy E. Auger collected now the largest number of hybrid events and we compare our predictions with the hybrid Auger data whenever this is possible.

At present TA is also using the hybrid technique with the help of 507 on-ground scintillation detectors [12]. With an accumulated statistics of 5 years data, TA reports [12] that the hybrid measurements of X_{max} agree with the results of Auger, if analysed with the EPOS-LHC hadronic interaction model [14]. On the other hand, using the QGSJet II-03 hadronic interaction model [15] the TA collaboration founds a mass composition compatible with only light nuclei.

Another important method to measure the mass composition is given by the observation of muons produced in the EAS.

The basic effect to distinguish a nucleus from a proton with the help of muons is related to the different energy per nucleon, E/A, at fixed total energy E. A low energy nucleon produces low energy charged pions which decay to muons before the parent pion undergoes new collisions with air-nucleus. Produced in the EAS, muons propagate rectilinearly with velocity $v \approx c$. As a result they can provide directional and timing informations, which can further reduce uncertainties in the fluorescent method. There are two well known muon quantities relevant for measuring mass composition: The total number of muons in the shower

N_μ and the so-called muon production depth (MPD) X^μ_{max}, which gives the atmospheric depth where the production rate of muons reaches its maximum [16–18].

The new exciting method of muon detection in Auger experiment is given by the Auger-Prime [19] upgrade, recently funded, has been specifically designed to improve muon detection in the whole energy range of the experiment. Each water-Cherenkov tank will be equipped with scintillator layer on the top, sensitive only to e-m component of the shower, while water-Cherenkov detector is sensitive to both e-m and muon components. The combination of the two signals allows to reconstruct each of the fluxes separately. Recently, also the TA collaboration started important upgrades to increase the statistics at the highest energies enlarging the area covered by the surface detectors, an updated description of the status of the TA experimental set-up can be found in [20].

In the present extended-abstract we use the latest Auger and TA observations, comparing them with the spectral features that arise due to propagation of UHECR, and their mass composition.

We argue that the spectral features may still be considered as an indication for a light mass composition, solving the problem of the alleged discrepancy between Auger and TA observations.

The extended-abstract is organised as follows: in Sec. 2 we show how a mixture of Helium nuclei and protons provide a good description of the observed flux. The conclusion is given in Sec. 3.

2. p + He MODEL

As discussed in the Introduction there is some tension on the mass composition at $E > 3$ EeV between the three biggest UHECR experiments Auger, TA and HiRes. In this Section we first summarise the basic physics of mass-composition measurements, then discuss the influence of cosmological environment and, finally, present calculations relevant to the p+He model.

The measurement of mass composition is based on the X_{max} value, which is the depth of the atmosphere where the number of particles in the shower reaches its maximum. The value of X_{max} is a basic parameter to determine the mass composition of UHECR, with the best observable quantity for this determination given by the shape of the distribution $N(X_{max}, E)$ for showers with fixed total energy E.

As a matter of fact, until recently, instead of the distribution $N(X_{max})$, the first two moments of this distribution were used: the mean value $\langle X_{max}\rangle$ and its RMS $\sigma(X_{max})$.

In two recent papers by the Auger collaboration, the mass-compositions obtained using moments-analysis [10] and shape-fitting $N(X_{max})$ analysis [11] are not identical. Realistically, they are not expected to be such, similarly to the already known fact that $\langle X_{max}\rangle$ and $\sigma(X_{max})$ give, if analysed separately, somewhat different results. The shape-fitting analysis is obviously the most fundamental and most sensitive method, since, for example, it involves the tiny parts of the wing distribution. Apart from it, the shape-fitting analysis demonstrated a degeneracy effect when two different mass compositions correspond to the same first two moments. For this reason, in the present paper, we choose the results obtained from the shape-fitting analysis of the Auger data [11] with the measured fractions of four nuclei species: Fe, N, He and p. These fractions, as determined from Auger measurements [11], reveal some uncertainties due to different hadronic interaction models namely QGSJet [15], EPOS-LHC [14] and Sibyll [21].

The important result obtained in [11] is given by a very small fraction of Iron at all energies and for all interaction models, except EPOS-LHC at the two highest energy bins (see the upper panel in Fig. 4 of [11]). The other important result, as mentioned in Introduction, and exposed in Fig. 1, is a large fraction of p+He, consistent with unity.

It is interesting to note that both effects have a natural cosmological explanation.

Among the heaviest nuclei, Iron is the most natural element to be produced in Supernova (SN) explosions and the absence of Iron in UHECR implies that other heavy elements must be absent too. Their suppression in the form $\mathrm{Fe}/p \ll 1$ is very natural for extragalactic gas and extragalactic cosmic rays. Enhancement of p + He component has the same nature.

At the cosmological epoch of recombination, protons and Helium nuclei were the dominant components and heavy metals were almost completely absent. Meanwhile, the production of metals is compulsory. It is needed to provide cooling of ordinary stars during their evolution, including the preSN phase. The later stage of reionization in the Universe, as detected by WMAP [22] and Planck [23] satellites occurs at redshift $z = 11.0 \pm 1.4$ and $z \lesssim 10.0$, respectively. This stage needs at least two early generations of stars with low metallicity, Pop III and Pop II stars. They inject into the extragalactic space a small amount of heavy metals. The main contribution to the Iron observed in the extragalactic space (and thus in extragalactic cosmic rays) is given by the present-time SN explosions. This scenario is confirmed by WMAP and Planck ob-

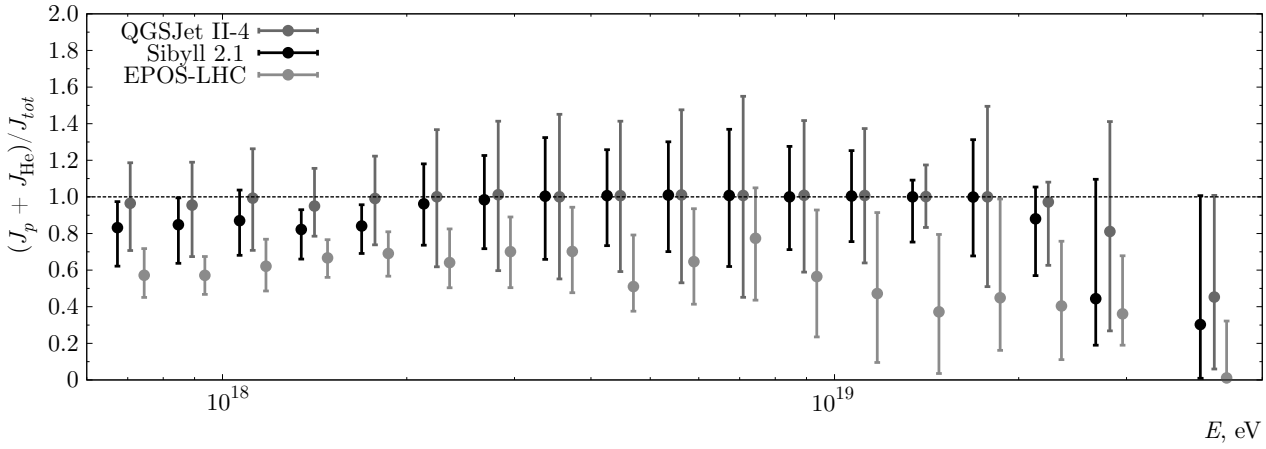

Fig. 1. (Color online) Fraction of $p + \mathrm{He}$ nuclei relative to the total one according to the Auger measurements [11] with error bars (summed in quadrature) taken from Fig. 4 of [11] using hadronic interaction models: Sibyll 2.1 (black), QGSJet II-4 (blue), and EPOS-LHC (red)

servations of the Universe reionization and by the observations of Lyα forest which indicate that extragalactic space had very low fraction of heavy elements at the level $Z \sim 10^{-3.5} Z_\odot$ at redshift $z \sim 5$, see e. g. [24]. Iron and other heavy metals are injected into extragalactic space mainly during a short interval Δz at $z \sim 0$ mostly due to explosions of the last generation of SNe. This scenario is similar to the model of UHECR produced mostly nearby our Galaxy [25].

One may conclude that Hydrogen and Helium as the main products of primordial cosmological nucleosynthesis, and suppression of SN-produced Iron and other heavy metals in red-shifted gas, naturally result in a $p + \mathrm{He}$ dominated extragalactic gas and UHECR accelerated at red-shift $z \geq$ a few.

In our calculations an additional simplifying assumption is used. Generically, we assume that all existing detectors do not distinguish reliably Helium from proton and one can consider $p + \mathrm{He}$ flux as a single light component, assuming the fraction He/p as a free parameter of the model. However, we will start with the sum $p + \mathrm{He}$ as it comes from Fig. 4 (strip 3 for He and strip 4 for p) of [11]. Summing these two fractions, with errors summed in quadrature, we obtain $p + \mathrm{He}$ flux presented in Fig. 1. One can see that the sum of these two components saturates well the total flux, at least in the case of QGSJet and Sibyll hadronic interaction models. This interesting fact confirms well our assumption that the light fraction ($p + \mathrm{He}$) weakly depends on energy and with good accuracy saturates the total flux leaving small room for other components (e. g. N which will be considered later as CNO component).

We are ready now to calculate the energy spectra for $p + \mathrm{He}$ models and to compare them with spectra released by Auger and TA in 2015. We consider a power-law generation spectrum as $Q(E) = K_i E^{-\gamma_g}$ ($i = p, \mathrm{He}$) with the same generation index γ_g for protons and Helium nuclei. We also assume that sources are distributed homogeneously and uniformly, so that the calculated spectrum is universal, i. e. not being affected by propagation models. Energy losses include pair-production, photo-pion production, and photo-dissociation for Helium on CMB and EBL.

Secondary protons from He and D photo-dissociation and also from neutron decays are included in calculations. For interaction with EBL photons the model [26] is used. In all these calculations we follow [27].

In Fig. 2 and Fig. 3 the computed spectra for $p + \mathrm{He}$ models are presented for $\gamma_g = 2.6$ and $\gamma_g = 2.2$, respectively. A generic feature of $p + \mathrm{He}$ spectra is the proton dominance at the highest energies because of the GR steepening for Helium at $E \lesssim 5 \cdot 10^{18}$ eV due to photo-disintegration on EBL. Therefore the GZK cutoff in $p + \mathrm{He}$ model becomes compulsory, unless the maximum acceleration energy E_{max}^{acc} is below the GZK threshold $E_{max}^{GZK} \simeq 50$ EeV.

Consider first the case of generation index $\gamma_g = 2.6$ shown in Fig. 2. This generation index corresponds to the canonical proton modification factor in the dip model [3–5]. Therefore if to take a small He/p ratio at generation one should obtain the theoretical spectrum and theoretical modification factor in agreement with old (before 2015) observations. One may notice from Fig. 2 the similar agreement between theoretical and observational dips for Auger 2015 (hybrid data) and

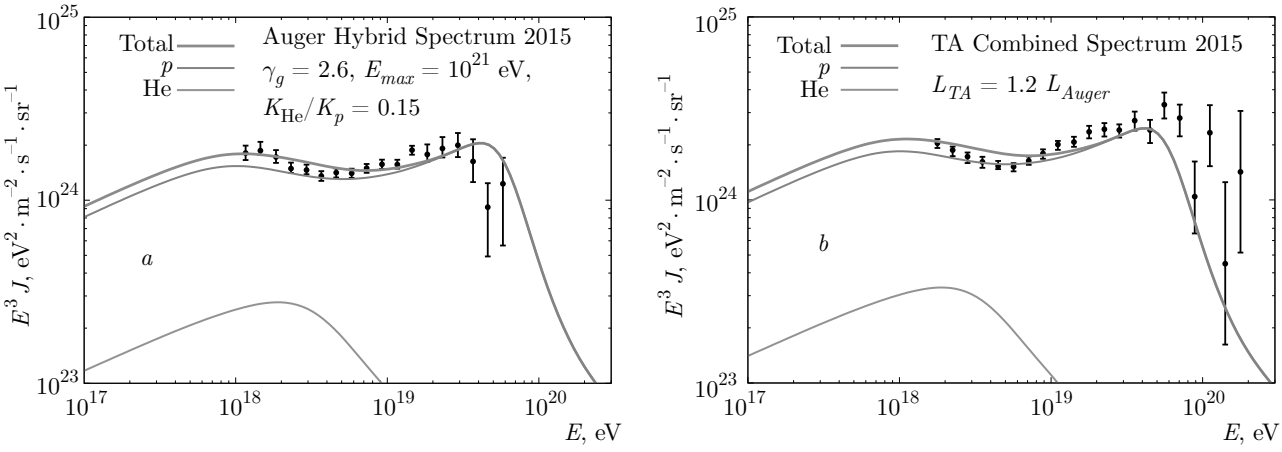

Fig. 2. (Color online) *a*) Energy spectrum for mixed p + He composition with injection index $\gamma = 2.6$, $E_{max}^{acc} = 10^{21}$ eV and He/$p = 0.15$ in the generation spectrum. The contribution of He is shown by magenta curves, proton by green and total by red. The calculated spectrum is compared with hybrid data of Auger 2015. *b*) As in panel *a* in comparison with TA combined data. The agreement needs a rescaling of the total flux by a factor 1.2. One may notice the excess of TA flux at energy above the GZK cutoff

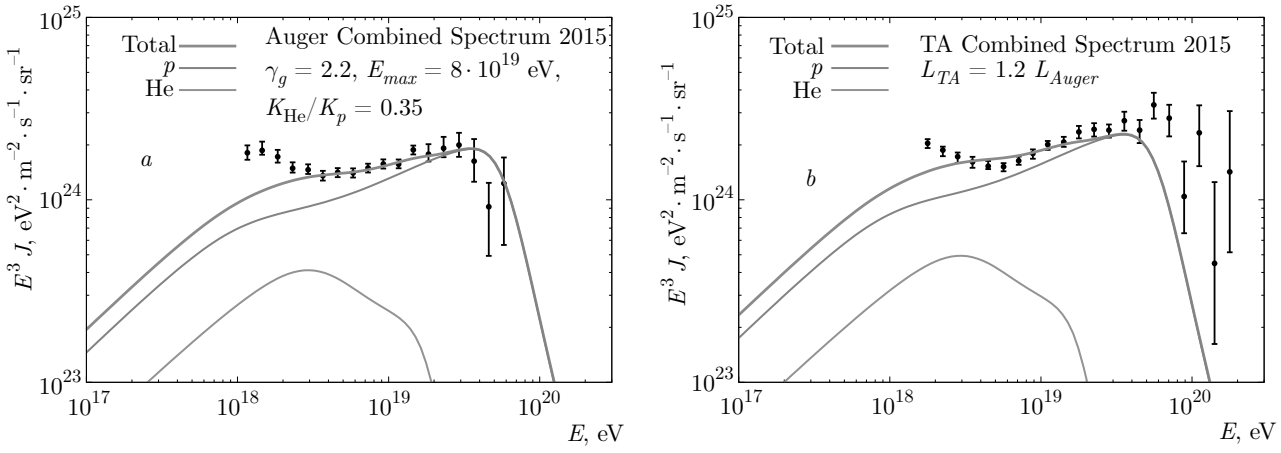

Fig. 3. (Color online) The same as in Fig. 2 but for $\gamma_g = 2.2$, $E_{max} = 8\cdot 10^{19}$ eV and a ratio of protons and Helium nuclei at the source He/$p = 0.35$

for TA 2015 (combined data). This agreement becomes worse at the highest energies.

In Fig. 2 we plot the comparison of the observed and calculated fluxes for Auger 2015 (*a*) and TA 2015 (*b*). It is remarkable that, at the dip energies, the TA spectrum can be described just rescaling by a factor 1.2, which is the source emissivity needed to describe the Auger data. The behavior of the flux at the highest energies is determined by the photo-pion production process. The maximum acceleration energy in Fig. 2 is taken at the level of $E_{max} = 10^{21}$ eV. In other words, the theoretical spectrum shape in Fig. 2 is exactly as predicted in the case of the GZK cutoff and, as follows from Fig. 2, it seems not well reproduced in both data sets. Auger shows an earlier cutoff at energies below the GZK cutoff energy ($\simeq 50$ EeV) while TA shows a flux suppression at energies slightly higher than this value.

The fraction of Helium allowed at the sources depends on the assumptions for the injection power-law index. Assuming harder spectra it is possible to increase the fraction of Helium. In Fig. 3 we assume a maximum acceleration energy $E_{max} = 8\cdot 10^{19}$ eV and a flatter injection spectrum with $\gamma_g = 2.2$, that allows to increase the fraction of Helium nuclei in the generation spectrum up to $K_{\rm He}/K_p = 0.35$. This procedure

improved but a little the agreement with observational data of Auger at the highest energies, while the good agreement with the dip remains practically as before. These changes are linked with the GR steepening of He spectrum due to photo-disintegration on the EBL radiation.

3. CONCLUSIONS

As far as mass composition is concerned there are three methods to analyse the fluorescence data: $\langle X_{max}\rangle$, $\sigma(X_{max})$ and the shape-fitting analysis of $N(X_{max})$ distribution [11]. As it is well known, the first two methods (moments of the X_{max} distribution) do not agree well between themselves and both disagree with the shape-fitting analysis (compare the mass composition obtained in [10] and in [11]). In this paper we used the Auger shape-fitting analysis as the most reliable and free from false degeneracies, see [11] and Introduction.

In the shape-fitting analysis the mass composition is described in terms of four nuclei species: p, He, N (we consider it as CNO) and Fe (which can be considered as Iron group including the heavy metals). The results of this analysis are given as fractions of the fluxes of these four elements, which depend rather strongly on the hadronic interaction models used. The new and important result of this analysis is the very small fraction of Iron, compatible with zero, practically for all models of hadronic interactions. We argue that this result is natural for the standard cosmology with reionization of the Universe.

Our first observation is that using QGSJet II-4 and Sibyll 2.1 for the hadronic interaction model the sum of protons and Helium nuclei fractions saturates with good precision the total flux, while for EPOS-LHC it leaves more space for other elements especially at the lowest and highest energies. Thus, a reasonable model could be a p + He dominated injection.

Next, we made the ad hoc assumption that at present all existing detectors cannot distinguish reliably Helium nuclei from protons and we calculated the spectra for Helium and protons considering them as a single component with the same injection power-law index γ_g equal to 2.6 and 2.2 and taking the ratio He/p at the source to fit the spectra of Auger and TA. These ratios are 0.15 for $\gamma_g = 2.6$ and 0.35 for $\gamma_g = 2.2$. The calculated spectra are shown in Figs. 2 and 3. The highest energy part of these spectra are always dominated by protons, because high-energy He nuclei are photo-disintegrated in collisions with EBL photons.

In the case of $\gamma_g = 2.6$ the observed dip is mainly produced by protons: it is the canonical case of the dip model [3–5].

In the case $\gamma_g = 2.2$ the dip at EeV energies of the spectrum is produced by both Helium and proton components. However, the observed high energy cutoff in the Auger spectrum is located at energy below the predicted GZK cutoff. In any case the shape of the spectrum alone is not enough to accept the model.

We conclude emphasising that the understanding reached so far on the mass composition of UHECR is still not conclusive. The observations of mass composition are still contradictory and cannot exclude a pure light composition, while the observations of spectra agree fairly well with such hypothesis. For these reasons the high energy muon program of Auger, especially the measurement of $X^{\mu}_{max}(E)$, will be a crucial test of the models discussed in this paper.

The full text of this paper is published in the English version of JETP.

REFERENCES

1. K. Greisen, Phys. Rev. Lett. **16**, 48 (1966); G. T. Zatsepin and V. A. Kuzmin, JETP Lett. **4**, 78 (1966).

2. G. R. Blumenthal, Phys. Rev. D **1**, 1596 (1970).

3. V. Berezinsky, A. Gazizov, and S. Grigorieva, Phys. Rev. D **74**, 043005 (2006).

4. V. Berezinsky, A. Gazizov, and S. Grigorieva, Phys. Lett. B **612**, 147 (2005).

5. R. Aloisio, V. Berezinsky, P. Blasi, A. Gazizov, S. Grigorieva, and B. Hnatyk, Astropart. Phys. **27**, 76 (2007).

6. T. Abu-Zayyad et al., Phys. Rev. Lett. **92**, 151101 (2004).

7. J. Abraham et al., Phys. Rev. Lett. **101**, 061101 (2008).

8. N. M. Gerasimova and I. L. Rozental, JETP **41**, 488 (1961).

9. R. Aloisio, V. Berezinsky, and S. Grigorieva, Astropart. Phys. **41**, 94 (2013).

10. A. Aab et al. (Auger Collaboration), Phys. Rev. D **90**, 122005 (2014).

11. A. Aab et al. (Auger Collaboration), Phys. Rev. D **90**, 122006 (2014).

12. R. U. Abbasi et al. (TA Collaboration), Astropart. Phys. **64**, 49 (2015).

13. T. Abu-Zayyad et al. (HiRes-MIA Collaboration), Astrophys. J. **557**, 686 (2001).

14. K. Werner, F. M. Liu, and T. Pirtoj, Phys. Rev. C **74**, 044902 (2006).

15. S. Ostapchenko, Phys. Rev. D **74**, 014026 (2006).

16. D. Garcia-Gamez et al. (Auger Collaboration), contribution ICRC 2011, arXiv:1107.4807.

17. R. Conceicao, S. Andringa, L. Cazon, and M. Pimenta (for the Auger Collaboration), EPJ Web Conf. **52**, 03004 (2013), arXiv:1301.0507.

18. L. Collica et al. (Auger Collaboration), Eur. Phys. J. Plus **131**, 301 (2016), arXiv:1609.02498.

19. A. Aab et al. (Auger Collaboration), *The Pierre Auger Observatory Upgrade — Preliminary Design Report*, arXiv:1604.03637.

20. R. U. Abbasi et al. (TA Collaboration), Astrophys. J. **858**(2), 76 (2018).

21. E. J. Ahn et al., Phys. Rev. D **80**, 094003 (2009).

22. G. Hinshaw et al. (WMAP Collaboration), Astrophys. J. Suppl. Ser. **180**, 225 (2009).

23. R. Adam et al. (Planck Collaboration), Astron. Astrophys. **596**, A108 (2016).

24. A. Songaila, Astrophys. J. **561**, L153 (2001).

25. R. Y. Liu, A. M. Taylor, X. Y. Wang, and F. A. Aharonian, Phys. Rev. D **94**, 043008 (2016); arXiv: 1603.03223.

26. F. W. Stecker, M. M. Malkan, and S. Scully, Astrophys. J. **648**, 774 (2006).

27. R. Aloisio, V. Berezinsky, and P. Blasi, JCAP **10**, 020 (2014).